Modeling Climate Dynamically

James Walsh and Richard McGehee

Jim Walsh (jawalsh@oberlin.edu) specializes in dynamical systems, having earned a Ph.D. from Boston University under the direction of G.R. Hall in 1991. His research interests increasingly center on applied dynamical systems and mathematical modeling. He is fortunate to have had the opportunity to spend a recent sabbatical at the University of Minnesota, participating in Richard McGehee's seminar on mathematics and climate. He is, above all, lucky to be the husband of Debbi and father of Zachary and Alexandra.

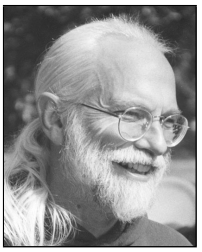

Richard McGehee (mcgehee@umn.edu) received a Ph.D. from the University of Wisconsin in 1969. Following a post-doctoral appointment at the Courant Institute of Mathematical Sciences, he joined the University of Minnesota faculty in 1970, where he has been ever since. He has held visiting positions at the ETH in Zurich, Switzerland, and at IMPA in Rio de Janiero, Brazil. He was also the Visiting Ulam Professor at the University of Colorado at Boulder. He is a founding member of the Mathematics and Climate Research Network (MCRN) and runs a research seminar on the mathematics of climate, which has been meeting weekly since 2007 and which is broadcast over the internet to participants throughout the country. His current research involves studying conceptual climate models as dynamical systems and comparing their behavior to the climate record.

Has the Earth ever been in a snowball state, its surface completely covered by glaciers? Short of this, have glaciers ever descended to tropical latitudes, leaving a narrow strip of open ocean water about the equator? Can mathematical models of climate accessible to undergraduates shed light on these possibilities?

Here, we present a dynamical systems approach to climate modeling by considering the questions posed above. Techniques from dynamical systems have recently proved successful in the study of climate, to the point of meriting an op-ed piece in the *New York Times* [**7**]. Our focus is on the insight the simplest energy balance models provide into the behavior of large scale aspects of climate, such as the position and movement of glaciers. Along the way, we highlight aspects of this approach appropriate for the undergraduate curriculum.

A global energy balance model

Energy balance models (EBM) are conceptual in nature, providing a broad view of the way in which a specified system variable, such as surface temperature, depends

http://dx.doi.org/10.4169/college.math.j.44.5.350
MSC: 34C60, 34C23

on a few prominent climate components. These models lie on the opposite end of the spectrum from highly sophisticated General Circulation Models (GCM) ([**5**], for example).

One advantage of EBM over GCM is the ease with which we can run simulations over long periods of time, as in the study of large-scale glacial cycles. Another is the focus we are able to place on individual factors and their influence on climate, a role assumed in this article by planetary albedo. Drawbacks include possible model sensitivity with regard to parameter values, which are often difficult to determine [**16**]. Additionally, fundamental processes such as cloud feedback and the hydrological cycle are typically not included in EBM [**15**, §9.2.6]. Nonetheless, the EBM mathematical modeling approach plays an important role in the study of climate, as succinctly stated by Gerald North [**13**]:

> Though the path to understanding global climate is obviously complicated, it is clear that mathematical modeling is the best starting point to test assumptions against geological and present day evidence.

Global climate is determined by the radiation balance of the planet. The Earth warms through the absorption of incoming solar radiation (or *insolation*). Due to the shortwave nature of radiation emitted by the sun, much of this energy passes freely through Earth's atmosphere. The Earth cools by radiating energy back into space, albeit at longer wavelengths, and some of this *Outgoing Longwave Radiation* (OLR) is absorbed by the atmosphere [**15**, chapter 3].

For the global climate model, the variable of interest is the annual global mean surface temperature $T = T(t)$ (°C). The annual global mean insolation is known as the *solar constant* Q, with current value $Q = 343$ W/m^2. The incoming energy absorbed by the Earth is then modeled by the term $Q(1 - \alpha)$, where α is the average global *albedo*, a measure of the extent to which shortwave insolation is simply reflected back into space.

The loss of energy via OLR is modeled by a linear approximation $A + BT$, with parameters A and B estimated from satellite measurements to be $A = 202$ W/m^2 and $B = 1.9$ W/(m^2 °C) [**6**]. The actual physics of the atmosphere is a complicated combination of thermodynamics and radiative transfer; the reader is referred to the thorough introduction provided in [**15**].

A model equation for the annual global mean temperature is then given by

$$R\frac{dT}{dt} = Q(1 - \alpha) - (A + BT). \tag{1}$$

The left-hand side of equation (1) represents the change in energy stored in the Earth's surface. The parameter R is the heat capacity of the Earth's surface, with units J/(m^2 °C). The units on each side of equation (1) are those of energy, namely W/m^2 (equivalently, J/(s m^2)).

We pause to comment on the use of annual averages in (1). The climate behavior modeled via EBM occurs on times scales of millennia. On this scale, it is reasonable to use annual averages for all variables and parameters. Since models are inherently approximations, a continuous time model such as (1) can serve as a reasonable approximation to the long-term behavior of climate components.

Equation (1) fits nicely into a sophomore-level ODE course or introductory dynamical systems course. A variant of this global mean temperature model with just this purpose is discussed in the Classroom Capsule by Köse and Kunze [**10**] in this issue starting on page 424. The reader is invited to show that, given any initial

condition $(t_0, T(t_0))$, the corresponding solution converges to the equilibrium value $T^* = \frac{1}{B}(Q(1-\alpha) - A)$. Letting α_w and α_s denote the albedo values for open water and snow-covered ice, respectively, we set $\alpha_w = 0.32$ and $\alpha_s = 0.62$ as in [**19**]. For an ice-free earth $\alpha = \alpha_w$, in which case a simple computation yields $T^* = 16.4°\text{C}$. If the Earth was covered by glaciers (the *snowball Earth* state), $\alpha = \alpha_s$, and T^* is a frosty $-37.7°\text{C}$.

The *critical temperature* at which we assume that glaciers are formed is typically taken to be $T_c = -10°\text{C}$, a figure based on observations of the modern climate. Given the parameter values above we see that, were the Earth ever in an ice-free state, no glaciers would form per this model. Similarly, if the Earth were ever in a snowball state, no ice would melt, and the planet would remain perpetually in a snowball state. Observing that we currently have glaciers that do not cover the entire globe, we might conclude that the Earth has never either been in the ice-free or snowball state. This contradicts the environment of, say, the early Eocene ($\sim$50 Mya (Million years ago)), when temperatures were so warm that alligators could be found above the artic circle [**9**]. It may also contradict the extreme glacial episodes of the Neoproterozoic Era, roughly 700 Mya, about which we will have more to say below.

Energy balance model: Latitude dependence

In seminal 1969 papers, M. Budyko [**3**] and W. Sellers [**17**] independently introduced EBM in which the surface temperature depends on latitude and time. In each model, the temperature is assumed constant on a given latitude circle. With θ as latitude, the variable $y = \sin\theta$ is convenient, representing, for example, the proportion of the Earth's surface between latitudes $\arcsin(-y)$ and $\arcsin(y)$. We refer to y as the "latitude" in what follows, trusting no confusion will arise on the reader's part.

For the Budyko–Sellers model, the temperature function, also called a *distribution* or *profile* and denoted $T = T(t, y)$ (°C), represents the annual average surface temperature at latitude y. As with the global model, we assume that this average varies continuously with time. We assume further that $T(t, y)$ is symmetric across the equator. It thus suffices to consider $y \in [0, 1]$, with $y = 0$ the equator and $y = 1$ the north pole. As a nice exercise, one can show the global annual average temperature is given simply by

$$\overline{T} = \overline{T}(t) = \int_0^1 T(t, y)\, dy. \tag{2}$$

Glaciers are incorporated into this model by an adjustment to the albedo function. We assume that ice exists above a given latitude $y = \eta$, while no ice exists below η. The parameter η is referred to as the *ice line*, with the albedo now a function $\alpha_\eta(y) = \alpha(y, \eta)$ depending on y and the position of the ice line η. As ice is more reflective than water or land, the albedo will be larger for latitudes above the ice line.

A second adjustment concerns the distribution of insolation. The tropics receive more energy from the sun on an annual basis than do the polar regions. This is taken into account by modeling the energy absorbed by the surface via the term

$$Qs(y)(1 - \alpha(y, \eta)),$$

where $s(y)$ represents the distribution of insolation over latitude, normalized so that

$$\int_0^1 s(y)\, dy = 1. \tag{3}$$

While $s(y)$ can be computed explicitly from astronomical principles [**11**], it is uniformly approximated to within 2% by the polynomial $s(y) = 1.241 - 0.723y^2$ [**14**]. We use $s(y) = 1.241 - 0.723y^2$ henceforth. Note that $s(y)$ is largest at the equator and decreases monotonically to a minimum at the north pole.

A final adjustment concerns *meridional heat transport*, encompassing physical processes such as the heat flux carried by the circulation of the ocean and the fluxes of water vapor and heat transported via atmospheric currents. We focus on Budyko's model, in which the meridional transport term is simply $C(T - \overline{T})$, with $\overline{T}$ as in (2) and C (W/m^2 °C) a positive empirical constant. Budyko's model is then

$$R\frac{\partial T}{\partial t} = Qs(y)(1 - \alpha(y, \eta)) - (A + BT) - C(T - \overline{T}). \tag{4}$$

The final term models the simple idea that warm latitudes (relative to the global mean temperature) lose heat energy through transport, while cooler latitudes gain heat energy.

While this model is, admittedly, inappropriate for that first differential equations course, its analysis fits nicely in a mathematical modeling course having an emphasis on computation.

Equilibrium solutions

As in the study of ODEs, we begin our treatment of (4) with the equilibrium solutions. An equilibrium solution $T^* = T^*(y, \eta)$ of (4) satisfies

$$Qs(y)(1 - \alpha(y, \eta)) - (A + BT^*) - C(T^* - \overline{T^*}) = 0. \tag{5}$$

Integration of each side of (5) with respect to y from 0 to 1, while recalling equation (3), yields

$$Q(1 - \overline{\alpha}(\eta)) - (A + B\overline{T^*}) = 0, \quad \text{where } \overline{\alpha}(\eta) = \int_0^1 s(y)\alpha(y, \eta)\, dy. \tag{6}$$

Solving for $\overline{T^*}$, we have the global mean temperature at equilibrium

$$\overline{T^*} = \overline{T^*}(\eta) = \frac{1}{B}(Q(1 - \overline{\alpha}(\eta)) - A). \tag{7}$$

Plugging this $\overline{T^*}$ into (5), and solving for T^*, we obtain

$$\begin{aligned} T^* = T^*(y, \eta) &= \frac{1}{B + C}\left(Qs(y)(1 - \alpha(y, \eta)) - A + C\overline{T^*}\right) \\ &= \frac{Q}{B + C}\left(s(y)(1 - \alpha(y, \eta)) + \frac{C}{B}(1 - \overline{\alpha}(\eta))\right) - \frac{A}{B}, \end{aligned} \tag{8}$$

with $\overline{\alpha}(\eta)$ as in equation (6). Given that we assume $s(y)$ and each of A, B, C, and Q are known, we see T^* (and hence $\overline{T^*}$) depends only on the albedo function $\alpha(y, \eta)$ and, in particular, on the position of the ice line.

Following Budyko, we consider first a 2-step albedo function

$$\alpha(y, \eta) = \begin{cases} \alpha_w, & y < \eta \\ \alpha_s, & y > \eta, \end{cases} \qquad \alpha_w = 0.32,\ \alpha_s = 0.62. \tag{9}$$

To find T^*, we compute $\overline{\alpha}(\eta)$:

$$\overline{\alpha}(\eta) = \int_0^\eta \alpha_w s(y)dy + \int_\eta^1 \alpha_s s(y)\,dy = \alpha_s - (\alpha_s - \alpha_w)(1.241\eta - 0.241\eta^3).$$

We can now use (8) to plot several equilibrium temperature profiles, as in Figure 1. For $\eta \in (0, 1)$, each of these profiles has a discontinuity at η due to our choice of $\alpha(y, \eta)$.

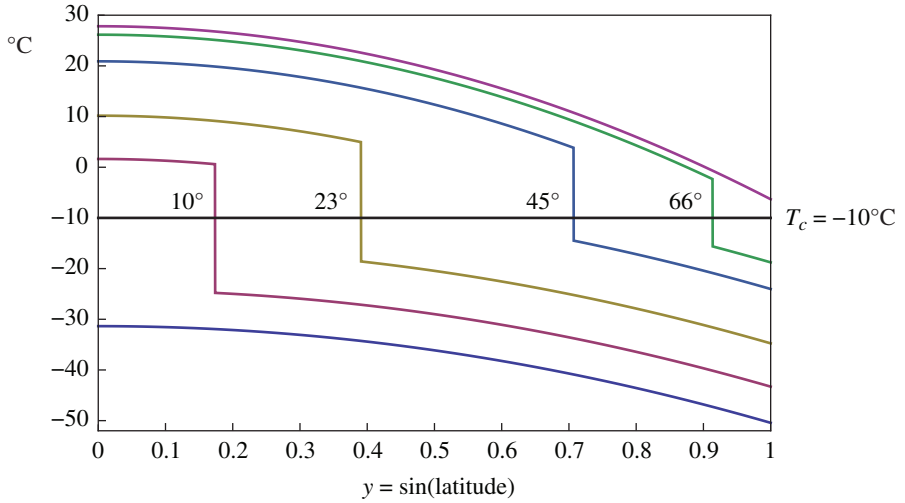

Figure 1. Equilibrium temperature profiles $T^*(y, \eta)$ with albedo $\alpha(y, \eta)$ as in equation (9). The bottom profile is for the snowball Earth. The top curve is for the ice-free state. Parameters: $A = 202$, $B = 1.9$, $C = 1.6B$, $Q = 343$, $\alpha_w = 0.32$, $\alpha_s = 0.62$.

In the ice-free state, $\alpha = \alpha_w$ for all y; we see from Figure 1 that the equilibrium temperature exceeds T_c at all latitudes y in this case. Hence, if the parameter values remain fixed, the planet never exits an ice-free state, as with the global Earth model. Similarly, $\alpha = \alpha_s$ for all y in the snowball state, and the equilibrium temperature at all latitudes y is less than T_c. Thus, if the Earth becomes completely ice covered, it once again remains so for all time.

Each specification of an ice line η yields an equilibrium temperature profile via equation (8). Put another way, there are infinitely many equilibrium functions, one for each $\eta \in [0, 1]$. What happens if we add the constraint that the temperature at the ice line at equilibrium must equal $T_c = -10°C$?

We define the temperature $T^*(\eta, \eta)$ at the ice line at equilibrium to be the average

$$h(\eta) = T^*(\eta, \eta) = \frac{1}{2}\left(\lim_{y\to\eta^-} T^*(y, \eta) + \lim_{y\to\eta^+} T^*(y, \eta)\right).$$

Using the continuity of $s(y)$, along with equations (8) and (9), a computation reveals

$$\begin{aligned} h(\eta) &= \frac{1}{B + C}\left(Qs(\eta)(1 - \alpha_0) - A + C\overline{T^*}\right), \\ &= \frac{Q}{B + C}\left(s(\eta)(1 - \alpha_0) + \frac{C}{B}(1 - \overline{\alpha}(\eta))\right) - \frac{A}{B}, \quad \alpha_0 = \frac{1}{2}(\alpha_w + \alpha_s). \end{aligned} \tag{10}$$

The plot of the function $h(\eta)$ in Figure 2 discloses the existence of two ice line positions $\eta_1, \eta_2 \in (0, 1)$, with $\eta_1 < \eta_2$ and $h(\eta_1) = -10^\circ\,\mathrm{C} = h(\eta_2)$. The corresponding equilibrium functions are also in Figure 2. Note that $T^*(y, \eta_1)$ corresponds to a very large ice cap, with mean global annual temperature a frigid $\overline{T^*}(\eta_1) = -21.4°\mathrm{C}$. The ice cap for $T^*(y, \eta_2)$ is closer to ours today, with $\overline{T^*}(\eta_2) = 14.9°\mathrm{C}$, a much more pleasant climate! We have more to say about these two equilibrium solutions shortly.

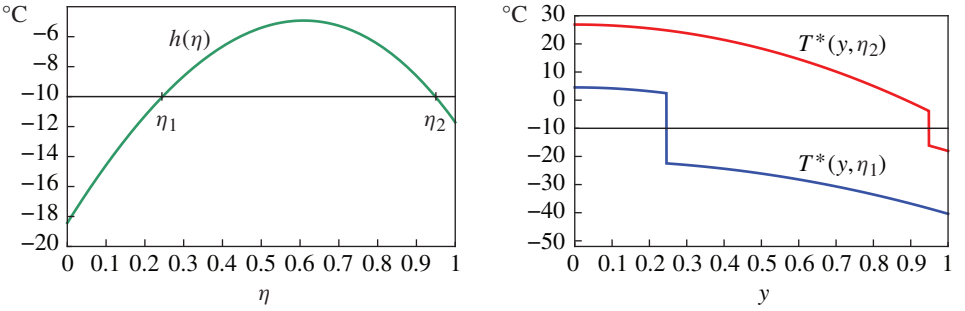

Figure 2. *Left.* Two ice line latitudes satisfying $h(\eta) = -10°\mathrm{C}$. *Right.* The corresponding equilibrium temperature profiles. Parameters as in Figure 1.

Bifurcations: A first pass

Equation (4) teems with parameters. In dynamical systems, we are often interested in how solutions change as one or more parameters vary. At this point we might investigate, for example, how the position η of the ice line at equilibrium changes as a parameter is varied. Budyko focused on the change in η at equilibrium as a function of Q (the solar "constant" varies significantly over long time scales), but we choose to keep all parameters fixed except A.

Recall that A is the constant in the term modeling OLR in equation (4). Carbon dioxide in our atmosphere interacts with radiation emitted by the Earth, strongly absorbing OLR in a range of spectral wavelengths [**15**, chapter 4]. We can thus think of A as a proxy for the amount of CO_2 in the atmosphere: An increase in CO_2 results in a decrease in OLR, which can be modeled by a decrease in A. Similarly, a decrease in atmospheric CO_2 results in an increase in OLR, and hence an increase in A.

A correspondence between the position η of the ice line at equilibrium and the parameter A can be realized by setting $h(\eta)$ from equation (10) equal to $-10°\mathrm{C}$ and solving for A. After a bit of algebra, we arrive at

$$A(\eta) = \frac{B}{B+C}\left(Qs(\eta)(1-\alpha_0) + \frac{C}{B}Q(1-\overline{\alpha}(\eta)) + 10(B+C)\right). \qquad (11)$$

We use (11) to generate the bifurcation diagram in Figure 3. The horizontal line at $\eta = 1$ corresponds to an ice-free planet, which occurs if the amount of CO_2 in the atmosphere is sufficiently large. In this scenario, OLR is trapped by the atmosphere to a great extent, leading to higher surface temperatures via the greenhouse effect [**15**, chapter 3]. Similarly, the line drawn at $\eta = 0$ corresponds to the snowball Earth state, which occurs for sufficiently low CO_2 values. The dotted vertical line in Figure 3

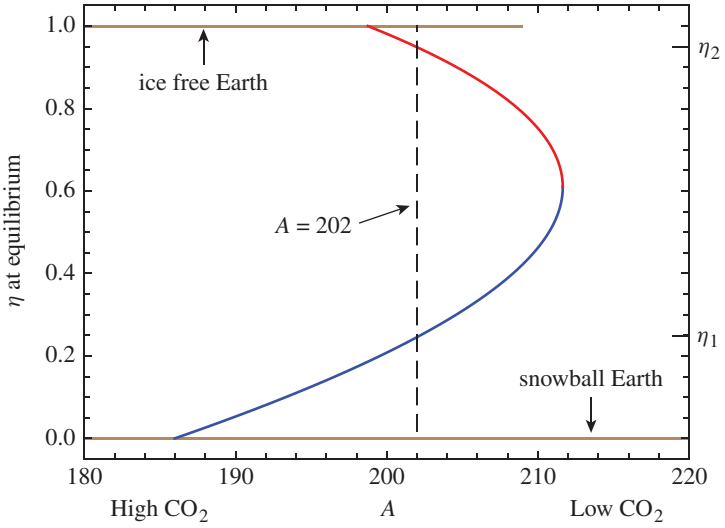

Figure 3. Position of the ice line η, satisfying $h(\eta) = -10°\text{C}$ at equilibrium for equation (4), as the parameter A varies. Remaining parameter values as in Figure 1. *Red*: Small ice cap. *Blue*: Large ice cap.

represents $A = 202$, for which the values $\eta_1 < \eta_2$, discussed previously and illustrated in Figure 2, satisfy $h(\eta_1) = -10°\text{C} = h(\eta_2)$.

Note the lack of equilibrium solutions with $h(\eta) = -10°\text{C}$ if $A > A_0 = 211.641$, while two such equilibrium solutions exist if A is slightly less than A_0. A_0 is found by maximizing $A(\eta)$ on $(0, 1)$. A *bifurcation* occurs at $A = A_0$, often called a *tipping point* in the climate science literature. If the CO_2 in the atmosphere decreases in such a way that A increases through A_0, runaway cooling occurs and the climate plunges into the snowball Earth state. This serves to illustrate positive *ice albedo feedback*: As A increases from $A = A_0$, more OLR escapes to space, the planet cools down, and the ice line descends toward the equator. Since more surface is now ice-covered, albedo increases, leading to further movement of the ice line toward the equator.

The above discussion is necessarily informal, as this model has no mechanism by which the ice line is allowed to move. Indeed, from both dynamical systems and modeling perspectives, the bifurcation diagram discussed above comes with an important caveat: There is no way to determine the *stability* of equilibrium solutions $T^*(y, \eta)$. Instead, there is an implicit assumption in previous interpretations of Budyko's model that the long-term behavior of solutions of (4) is determined by the equilibrium solutions.

A simple example that this need not be the case is the damped pendulum. The inverted and straight downward positions are equilibrium solutions; the former is unstable (solutions starting nearly vertical move away from the vertical when released); the latter is an attracting equilibrium (solutions that start nearly downward approach the straight downward equilibrium over time). The unstable equilibrium plays no (or, at best, very little) role in determining the dynamics of the model.

Budyko and several subsequent authors did investigate stability issues related to the position of η at equilibrium as a function of a parameter (typically Q; see [**4**], for example). This again begs the mathematical question, however, of whether solutions to (4) approach $T^*(y, \eta)$ for given, fixed parameter values, in spirit akin to the damped pendulum converging to the downward position over time.

The stability type of equilibrium solutions $T^*(y, \eta)$ has been rigorously established only recently [**21**]; we turn now to this result, along with the requisite model enhancement, prior to returning to bifurcations.

The Budyko–Widiasih model: A dynamic ice line

It is reasonable to expect the ice line to move in response to changes in the surface temperature. E. Widiasih [**21**] used this idea to enhance Budyko's model by creating the system

$$\begin{aligned} R\frac{\partial T}{\partial t} &= Qs(y)(1-\alpha(y,\eta)) - (A+BT) - C(T-\overline{T}) \\ \frac{d\eta}{dt} &= \epsilon(T(\eta,\eta) - T_c), \end{aligned} \tag{12}$$

where $\epsilon > 0$. Given a temperature profile $T(y, \eta)$, we check the temperature $T(\eta, \eta)$ at the ice line. If $T(\eta, \eta)$ is less than T_c, ice forms and the ice line descends, while the ice line moves poleward if $T(\eta, \eta) > T_c$. Motivated by paleoclimate data, McGehee and Widiasih [**12**] proposed a value for ϵ on the order of 10^{-13}. The size of ϵ reflects the idea that the ice sheets move very slowly in response to changes in temperature.

Equilibrium solutions for (12) consist of pairs $(T^*(y, \eta), \eta)$ for which $T^*(y, \eta)$ satisfies both equation (4) and $T^*(\eta, \eta) = -10°\text{C}$. Recall, for example, that there are precisely two such solutions for A between roughly $A = 199$ and $A = 211$ when $\epsilon = 0$, as indicated in Figure 3.

In a highly technical work involving tools from analysis and dynamical systems, Widiasih proved that, for sufficiently small ϵ, the dynamics of system (12) is well approximated by solutions to the single ODE

$$\frac{d\eta}{dt} = \epsilon(h(\eta) - T_c), \tag{13}$$

with $h(\eta)$ as in equation (10). The reader is referred to [**21**] for a precise statement of this result.

We refer to Figure 2 to interpret Widiasih's Theorem. For $\eta \in (\eta_2, 1)$, $h(\eta) < -10°\text{C}$, and we conclude from equation (13) that η decreases. Thus, the ice line descends as new ice forms. Alternatively, for $\eta \in (\eta_1, \eta_2)$, $h(\eta) > -10°\text{C}$ and the ice line moves poleward as the ice melts. We conclude that η_2 corresponds to an *attracting equilibrium solution* of system (12) (with a corresponding equilibrium temperature profile T^*).

Similarly, $h(\eta) < -10°\text{C}$ for $\eta \in (0, \eta_1)$, forcing the ice line to move equatorward for these latitudes, and we see that η_1 corresponds to an *unstable rest point* for system (12). Hence, the small ice cap is a stable solution, while the large ice cap is unstable. Note that equation (13) can be analyzed qualitatively by students in the first ODE course with the aid of technology, simply by sketching and interpreting the graph of $h(\eta)$ as we have done.

A dynamical bifurcation diagram

The Budyko–Widiasih model is on solid ground from a dynamical systems point of view. We can now incorporate model dynamics in redrawing the bifurcation diagram,

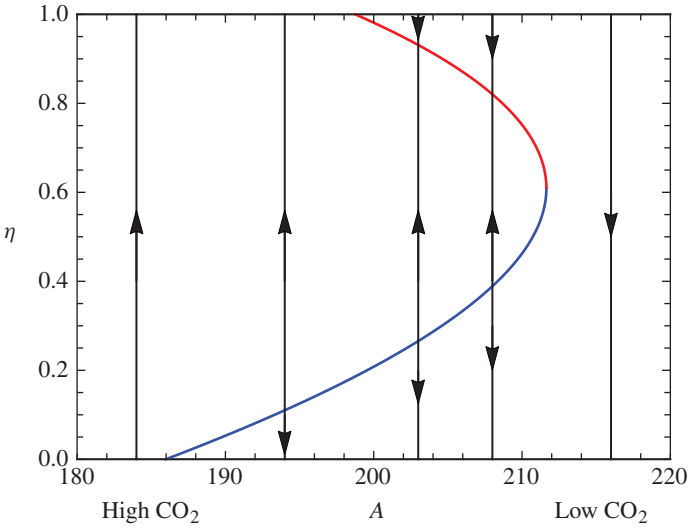

Figure 4. Dynamic bifurcation diagram for the Budyko–Widiasih model (12). Arrows indicate the movement of the ice line as solutions evolve. *Red*: Stable equilibrium. *Blue*: Unstable equilibrium.

originally of Figure 3. This dynamic bifurcation diagram (Figure 4) is of the type discussed in introductory differential equations texts such as [**2**].

Widiasih succeeded in incorporating the equator ($\eta = 0$) and the north pole ($\eta = 1$) in her reduction to equation (13), concluding that the ice-free state is now unstable, while the snowball Earth state remains stable, for a range of A values. This follows in essence from Figure 2, by observing that $h(1) < -10°\text{C}$ and $h(0) < -10°\text{C}$ (see [**21**] for details).

A second remark concerns the 2-step albedo function $\alpha(y, \eta)$, which in Widiasih's analysis is required to be continuous. A typical continuous approximation to the albedo function of equation (9) is

$$\alpha(y, \eta) = \frac{1}{2}(\alpha_s + \alpha_w) + \frac{1}{2}(\alpha_s - \alpha_w) \tanh M(y - \eta), \tag{14}$$

where M controls the sharpness of the transition from open water to ice (see Figure 5). The equilibrium temperature profiles $T^*(y, \eta)$ are now continuous at η when using (14), while the qualitative nature of the graph of $h(\eta)$ in Figure 2 remains the same [**21**]. In particular, the model still produces a small stable ice cap and a large unstable ice cap. The use of equation (14) does force us to use technology to sketch equilibrium solutions and bifurcation diagrams, however, because $\overline{\alpha}(\eta)$ becomes more of a challenge to compute.

The behavior of solutions to system (12) is intimately connected to the qualitative nature of the albedo function. We have seen that an albedo function $\alpha(y, \eta)$ with essentially one value on each side of the ice line leads to two equilibria, one attracting, the other unstable. Might the Budyko–Widiasih model, with an appropriate adjustment to $\alpha(y, \eta)$, be capable of modeling the great glacial episodes of the Neoproterozoic Era?

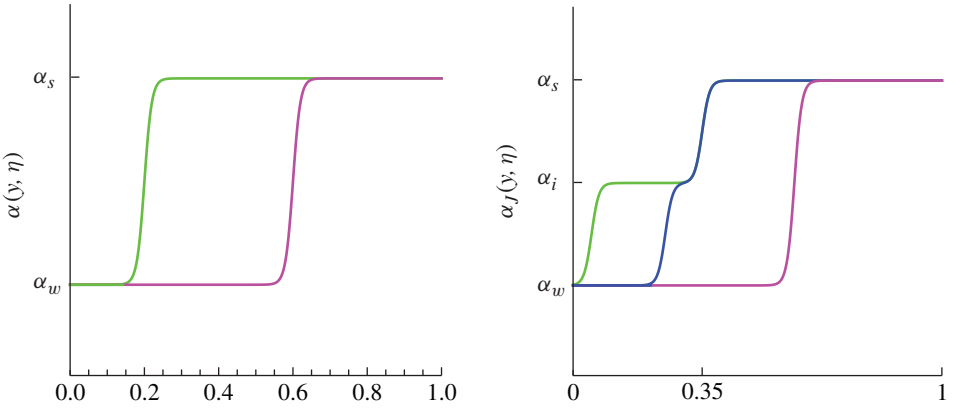

Figure 5. *Left.* The albedo function (14). Green: $\eta = 0.2$. Magenta: $\eta = 0.6$. *Right.* The albedo for the Jormungand model. *Green*: $\eta = 0.05$. *Blue*: $\eta = 0.25$. *Magenta*: $\eta = 0.6$.

Extreme glacial events of the past

The web supplies much information on "snowball Earth" (the interested reader might start at [**18**]). A wealth of geological and geochemical evidence suggests that ice sheets flowed into the ocean near the equator during two Neoproterozoic glacial periods, roughly 630 Mya and 715 Mya ([**1, 8, 16**], and their references).

Many support the occurrence of snowball Earth; others believe the descent of the glaciers halted before reaching the equator. There is evidence, for example, suggesting that photosynthetic eukaryotes, and perhaps certain types of sponges, thrived both before and in the aftermath of these glacial episodes. This, in turn, led to the proposal of the *Jormungand* or *Waterbelt* global climate state [**1**], an alternative to the snowball Earth hypothesis. In the Jormungand climate, the glaciers descend to tropical latitudes without triggering a runaway snowball Earth event. In this way, sunlight can reach organisms in the ocean in a band of open water about the equator.

The Jormungand model

Sea ice will be covered with snow, provided there is sufficient precipitation. Using the albedo effect of clouds in the atmosphere above the tropics, as well as atmospheric circulation considerations, an argument is made in [**1**] for net evaporation in a tropical latitude band during the cold climate of the Neoproterozoic glacial periods. Hence, new sea ice forming in this band would remain bare due to insufficient precipitation, relative to evaporation. Bare sea ice has an albedo greater than that of open water, but less than that of snow-covered ice. In particular, as bare sea ice absorbs more insolation than does snow-covered ice, the existence of this band furnishes a potential mechanism by which the advance of the glaciers might be halted prior to reaching the equator.

A bare sea ice albedo α_i, with $\alpha_w < \alpha_i < \alpha_s$, is thus included in the albedo function for the Jormungand climate model. The ice line η will continue to be regarded as the boundary between open water and (in this case bare) sea ice. As in [**1**], we assume that no bare sea ice exists above $y = 0.35$. Thus for $\eta \geq 0.35$, there is only open water and snow-covered sea ice, as before. The albedo function α_J has three "steps," however, corresponding to α_w, α_i, and α_s, for $\eta < 0.35$. Looking to apply Widiasih's result, we supply such a continuous albedo function $\alpha_J(y, \eta)$ in Figure 5. This function is

designed so that the extent of the bare sea ice decreases linearly from 0.35, when $\eta = 0$, to zero when $\eta \geq 0.35$. A snowball Earth, for example, now has bare sea ice extending from the equator to latitude $y = 0.35$, and snow-covered ice north of $y = 0.35$. A formula for such an α_J is provided in [**20**].

The use of α_J in system (12) requires the new computation

$$\overline{\alpha_J}(\eta) = \int_0^1 \alpha_J(y, \eta) s(y)\, dy$$

in the analysis. This can be accomplished by *Mathematica* or MATHLAB. A few of the resulting equilibrium temperature profiles $T_J^*(y, \eta)$ of equation (4) are sketched in Figure 6. We can show that Widiasih's result can be applied to reduce system (12) to the study of the analog of equation (13), one with $h(\eta)$ replaced by

$$h_J(\eta) = \frac{Q}{B + C}\left(s(\eta)(1 - \alpha_J(\eta, \eta)) + \frac{C}{B}(1 - \overline{\alpha_J}(\eta))\right) - \frac{A}{B}, \tag{15}$$

for the Jormungand model [**20**]. We can then numerically compute and graph the function $h_J(\eta)$, as in Figure 7.

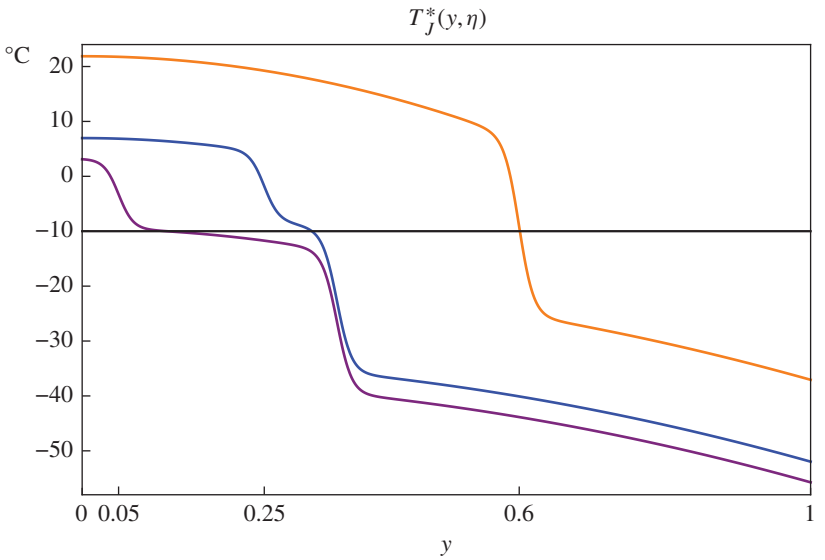

Figure 6. Equilibrium solutions $T_J^*(y, \eta)$ of equation (4) with the Jormungand model albedo of Figure 5. *Purple*: $\eta = 0.05$, *blue*: $\eta = 0.25$, *orange*: $\eta = 0.6$.

Parameter values appropriate to the Neoproterozoic Era are difficult to specify. It is known that the solar constant Q was 94% of its current value 700 Mya. As in [**1**], we assume meridional heat transport was less efficient due to the very cold climate, thereby reducing the value of C. Moreover, due to the massive ice sheets, the drawdown of CO_2 from the atmosphere via silicate weathering [**15**] was reduced, potentially leading to smaller values of A and B. Albedo values for the various surface components are difficult to specify as well. Admittedly then, following the lead of [**1**], we fiddled with the parameters a bit to get the desired $h_J(\eta)$ graph.

The plot in Figure 7 indicates that there are three equilibrium solutions, with ice lines $\eta_1 < \eta_2 < \eta_3$ satisfying $h_J(\eta_i) = -10°\text{C}$, $i = 1, 2, 3$. As in the previous analysis, η_3 corresponds to a small stable (attracting) ice cap, while η_2 is unstable. However,

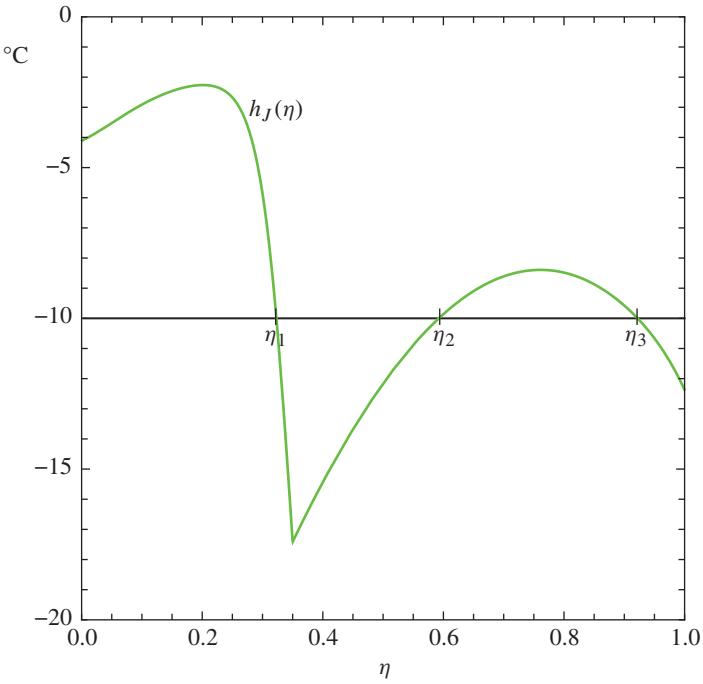

Figure 7. System (12) admits three equilibrium solutions with $h_J(\eta_i) = -10°\text{C}$, $i = 1, 2, 3$, in the Jormungand model with albedo function $\alpha_J(y, \eta)$ of Figure 5. Parameters: $A = 180$, $B = 1.5$, $C = 2.25$, $Q = 321$, $\alpha_w = 0.32$, $\alpha_i = 0.44$, $\alpha_s = 0.74$.

as $h_J(\eta)$ is greater than $-10°\text{C}$ on $(0, \eta_1)$, ice melts in this region and the ice line moves toward η_1. As $h_J(\eta)$ is less than $-10°\text{C}$ on (η_1, η_2), ice forms in this region, and again the ice line moves toward η_1. We conclude that η_1 corresponds to an attracting equilibrium solution of system (12), one with an ice line in tropical latitudes. In addition, while the ice-free state is once again unstable ($h_J(1) < -10°\text{C}$), the snowball Earth state becomes unstable ($h_J(0) > -10°\text{C}$) in the Budyko–Widiasih rendering of the Jormungand model.

A dynamically resolved bifurcation diagram for the Jormungand model is presented in Figure 8. The phase line at $A = 180$ in Figure 8 corresponds to the graph of $h_J(\eta)$ in Figure 7. For a range of A values (roughly between 176.5 and 182), system (12) admits both small and large stable ice caps, with an intermediate unstable ice cap. As A increases through roughly $A = 182$ (so that atmospheric CO_2 decreases), the small equilibrium ice cap disappears and solutions now converge to an equilibrium having a large stable ice cap. A second tipping point occurs near $A = 191.5$ when the large ice cap vanishes, resulting in a runaway snowball Earth event.

A final bifurcation occurs when A decreases through $A = 169$, at which point the large ice cap disappears and the system heads toward the ice-free state. We see that a simple adjustment to the albedo function has led to a remarkable change in the behavior of the energy balance model.

Conclusion

The study of climate presents enormous challenges. Energy balance models lie on the conceptual, or low-order, end of the modeling spectrum, focusing on a few major

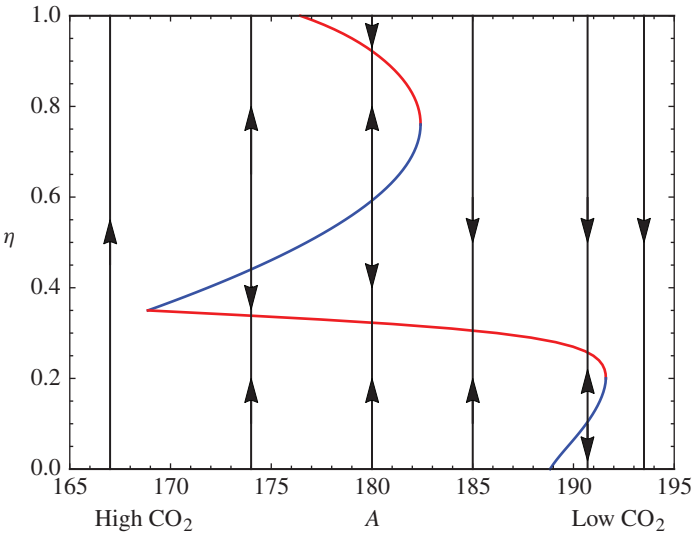

Figure 8. Dynamic bifurcation diagram for the Jormungand model. Arrows indicate the movement of the ice line as solutions to system (12) evolve, with albedo function $\alpha_J(y, \eta)$. *Red*: Stable equilibrium, *blue*: Unstable equilibrium.

elements of climate systems. It is decidedly not the role of EBM to provide detailed predictions of climate, even on a planetary scale. However, such models can provide a broad view of the role played by crucial climate components. Based on the Budyko–Sellers and Budyko–Widiasih models, for example, we have gained insight here into the sensitivity of climate to changes in albedo.

We highlighted Widiasih's theorem [**21**] to provide an example of the success dynamical systems has had in the arena of climate modeling. As [**21**] requires continuous versions of model-appropriate albedo functions (e.g., (14)), a student encountering this material in a mathematical modeling course would need technology to compute equilibrium temperature profiles, bifurcation diagrams, and investigate model sensitivity to changes in parameters. There is, however, a wealth of material in climate modeling at the level of EBM appropriate for students in such a computational modeling course.

The interaction of science and mathematics in the study of climate is also noteworthy. The physics of blackbody radiation, the chemistry of the greenhouse effect, the carbon cycle—there is an inherent cross-disciplinary appeal to this material. From mathematical and computational modeling perspectives, the study of energy balance models offers many possibilities for exploration by undergraduates.

Summary. A dynamical systems approach to energy balance models of climate is presented, focusing on low order, or conceptual, models. Included are global average and latitude-dependent, surface temperature models. The development and analysis of the differential equations and corresponding bifurcation diagrams provides a host of appropriate material for undergraduates.

References

1. D. Abbot, A. Viogt, and D. Koll, The Jormungand global climate state and implications for Neoproterozoic glaciations, *J. Geophys. Res.* **116** (2011) (D18103); available at http://geosci.uchicago.edu/~abbot/PAPERS/abbot-et-al-11.pdf.

2. P. Blanchard, R. Devaney, and G. R. Hall, *Differential Equations*, 4th ed., Cengage, 2011.
3. M. I. Budyko, The effect of solar radiation variation on the climate of the Earth, *Tellus* **5** (1969) 611–619.
4. R. Cahalan and G. North, A stability theorem for energy-balance climate modes, *J. Atmos. Sci.* **36** (1979) 1178–1188; available at http://dx.doi.org/10.1175/1520-0469(1979)036<1178:ASTFEB>2.0.CO;2.
5. Community Earth System Model, National Center for Atmospheric Research; see http://www2.cesm.ucar.edu/.
6. C. Graves, W-H. Lee, and G. North, New parameterizations and sensitivities for simple climate models, *J. Geophys. Res.* **198** (D3) (1993) 5025–5036.
7. F. Guterl, Searching for clues to calamity, *New York Times*, July 21, 2012, A19.
8. P. Hoffman and D. Schrag, The snowball Earth hypothesis: testing the limits of global change, *Terra Nova* **14** (3) (2002) 129–155; available at http://dx.doi.org/10.1046/j.1365-3121.2002.00408.x.
9. P. Jardine, Patterns in palaeontology: the Paleocene–Eocene thermal maximum, *Paleontology* [online] **1** (5) (2011) 2–7; available at http://www.palaeontologyonline.com/articles/2011/the-paleocene-eocene-thermal-maximum/.
10. E. Köse and J. Kunze, Climate modeling in the calculus classroom, *College Math. J.* **44** (2013) 424–427.
11. R. McGehee and C. Lehman, A paleoclimate model of ice-albedo feedback forced by variations in Earth's orbit, *SIAM J. Appl. Dyn. Syst.* **11** (2) (2012) 684–707; available at http://dx.doi.org/10.1137/10079879X.
12. R. McGehee and E. Widiasih, A finite dimensional version of a dynamic ice-albedo feedback model, preprint.
13. G. North, Analytical solution to a simple climate model with diffusive heat transport, *J. Atmos. Sci.* **32** (1) (1975) 1301–1307; available at http://dx.doi.org/10.1175/1520-0469(1975)032<1301:ASTASC>2.0.CO;2.
14. ———, Theory of energy-balance climate models, *J. Atmos. Sci.* **32** (11) (1975) 2033–2043; available at http://dx.doi.org/10.1175/1520-0469(1975)032<2033:TOEBCM>2.0.CO;2.
15. R. Pierrehumbert, *Principles of Planetary Climate*, Cambridge University Press, New York, 2010.
16. R. Pierrehumbert, D. Abbot, A. Voigt, and D. Koll, Climate of the Neoproterozoic, *Annu. Rev. Earth Planet. Sci.* **39** (May 2011) 417–460; available at http://dx.doi.org/10.1146/annurev-earth-040809-152447.
17. W. Sellers, A global climatic model based on the energy balance of the Earth-Atmosphere system, *J. Appl. Meteor.* **8** (1969) 392–400; available at http://dx.doi.org/10.1175/1520-0450(1969)008<0392:AGCMBO>2.0.CO;2.
18. Snowball Earth; see http://www.snowballearth.org/.
19. K. K. Tung, *Topics in Mathematical Modeling*, Princeton University Press, Princeton, NJ, 2007.
20. J. A. Walsh and E. Widiasih, A dynamics approach to low order climate models, to appear in *Discrete and Continuous Dynamical Systems Series B.*
21. E. Widiasih, Instability of the ice free Earth: dynamics of a discrete time energy balance model, to appear in *SIAM J. Appl. Dyn. Syst.*

Joseph Fourier on the Greenhouse Effect

Although he did not use the term, Fourier was aware of the greenhouse effect in the early 1800s. In his article on global temperature, "Mémoire sure les températures du globe terreste et des espace planétaires" (in *Mémoire de l'Académie Royale des Sciences* **7** (1827), 569–604, reprinted in *The Warming Papers: The Scientific Foundation for the Climate Change Forecast*, edited by David Archer and Raymond Pierrehumbert, Wiley-Blackwell, 2011), he describes a device for demonstrating the effect, a miniature greenhouse invented by Horace Bénédict de Saussure,

> The experiment consists of exposing a vessel covered by one or more sheets of highly transparent glass. . . to the rays of the sun. . . . Thermometers placed within the gaps between the sheets of glass indicate a much lower degree of heat acquired decreasing steadily from the bottom of the box up to the top gap.

—Suggested by Richard McGehee and James A. Walsh